Towards an Integrated ELM model

Howard Wilson

Thanks to Steve Cowley, Andrew Kirk and Phil Snyder for contributions

Culham Science Centre, Abingdon, Oxon OX14 3DB UK

Supported by the UK Engineering and Physical Sciences Research Council and EURATOM,

Outline

Ideal MHD stability boundaries for the pedestal

A “picture” of the ELM

Linear Ideal MHD stability properties

the ELM trigger

Non-linear ballooning mode structure

The structure of the ELM

An integrated ELM model

The essential ingredients: what is missing?

Summary

Ideal MHD Instabilities

There are two main drives for ideal MHD instabilities:

pressure gradient ⇒ ballooning modes

current gradient ⇒ kink, or peeling, modes

$$\delta W = \pi \int_0^{\psi_a} d\psi \oint d\theta \left\{ \frac{JB^2}{R^2 B_p^2} \left| k_{\|} X \right|^2 + \frac{R^2 B_p^2}{JB^2} \left| \frac{1}{n} \frac{\partial}{\partial \psi} \left(JBk_{\|} X \right) \right|^2 \right.$$

Field-line bending: strongly stabilising unless $k_{\|}$ is small

$$\frac{-2J}{B^2} \frac{dp}{d\psi} \left[\left| X \right|^2 \frac{\partial}{\partial \psi} \left(p + \frac{B^2}{2} \right) - \frac{i}{2} \frac{f}{JB^2} \frac{\partial B^2}{\partial \theta} \frac{X^*}{n} \frac{\partial X}{\partial \psi} \right]$$

Pressure gradient/curvature drive: destabilising if average curvature is "bad"

$$\left. - \frac{X^*}{n} JBk_{\|} \left(\frac{\partial \sigma}{\partial \psi} X \right) + \frac{\partial}{\partial \psi} \left[\frac{\sigma}{n} X JBk_{\|}^* X^* \right] \right\}$$

Kink drive

Peeling drive

Current density gradient/edge current drives kink/peeling modes

σ=normalised current density

In the pedestal region, large pressure gradients can build up

directly drives ballooning modes

drives bootstrap current ⇒ kink, or peeling, modes

Stability influenced by current and pressure

	Peeling mode	Ballooning mode
Current	Destabilising	Stabilising
Pressure	Stabilising	Destabilising
Radial extent	Highly localised	Extended across pedestal region

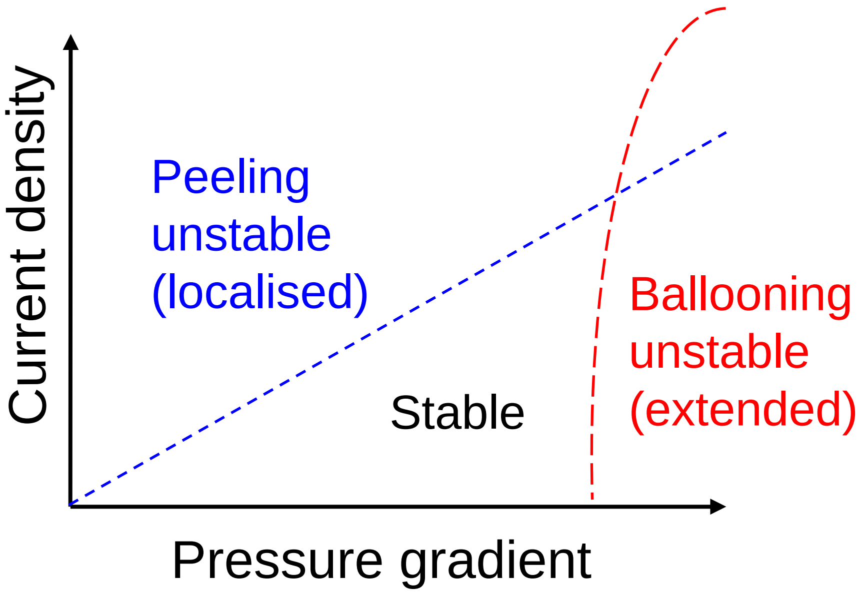

A model for the ELM cycle: the peeling ballooning model

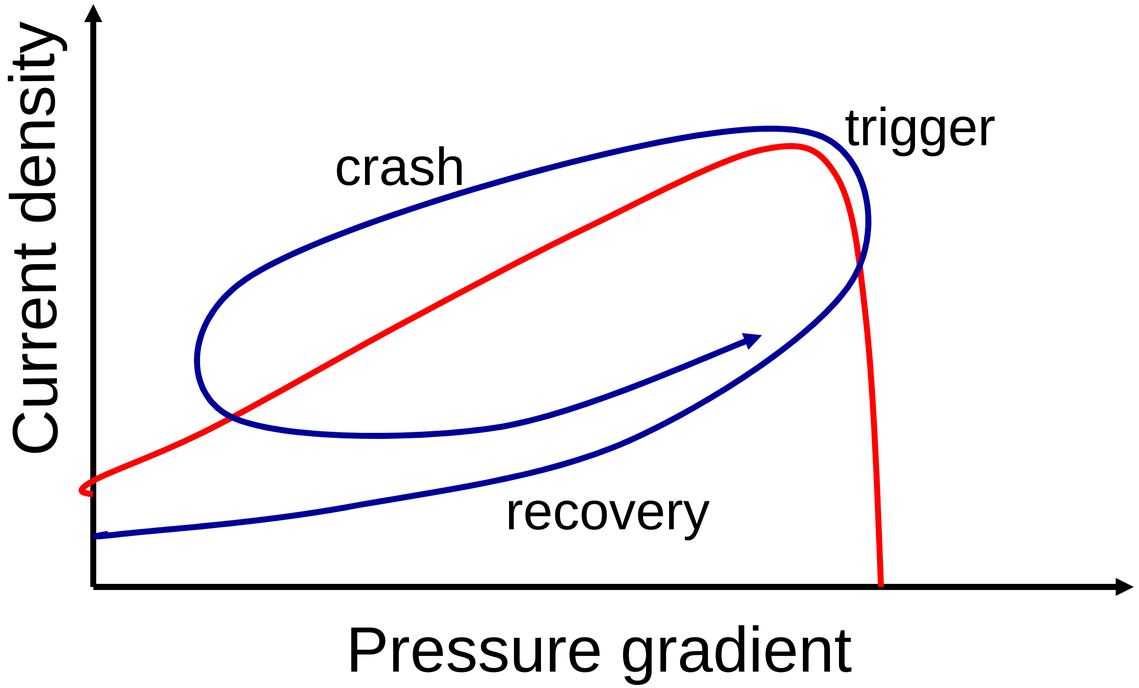

The ELM Triangle

- It is important to understand each element of the ELM triangle
  - To understand how to access small ELM regimes
  - To understand how to control ELMs
- A complete ELM model must involve the integration of all stages
  - A range of different physics phenomena are involved
- We shall address some of the issues involved in such an integrated model

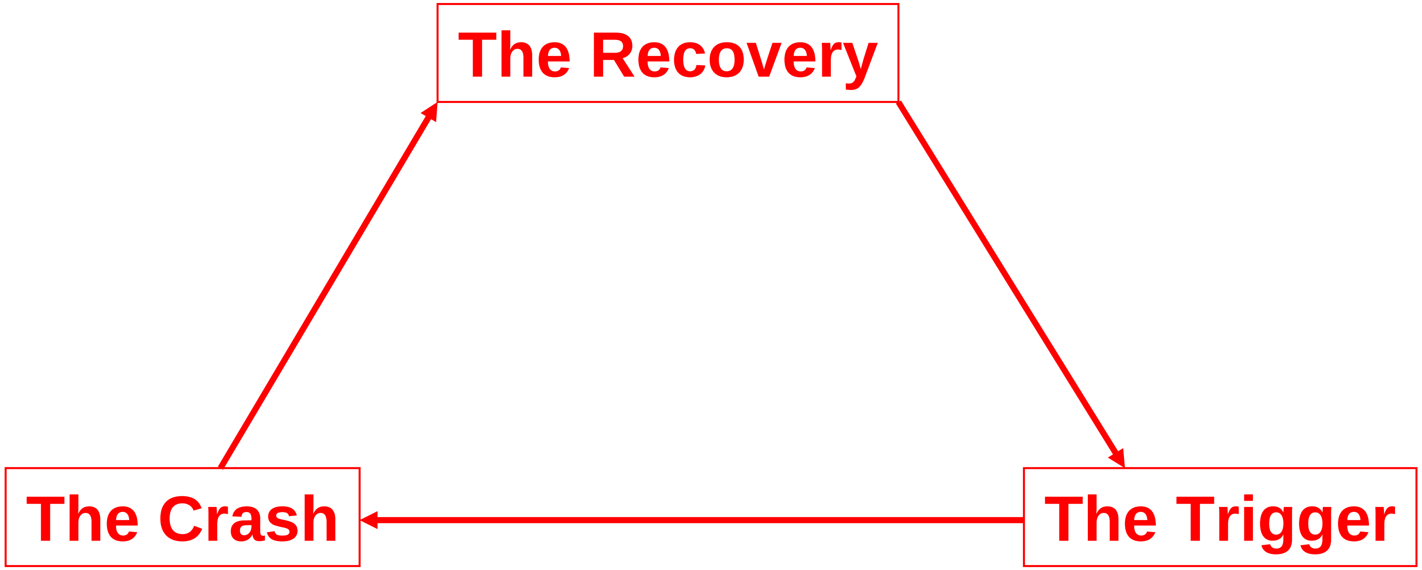

The Recovery: Largely understood?

- Important as it determines the ELM frequency
- Presumably “simply” a transport model issue
- Thus, a transport model is a key ingredient, but even here there are open questions:
  - What processes govern the transport in the pedestal region?
  - Is current diffusion neoclassical or anomalous? (could be important if edge current density plays a role in the ELM trigger)
  - Is standard neoclassical theory applicable in the pedestal region?

The linear theory can provide the trigger and, possibly a qualitative model for ELM size

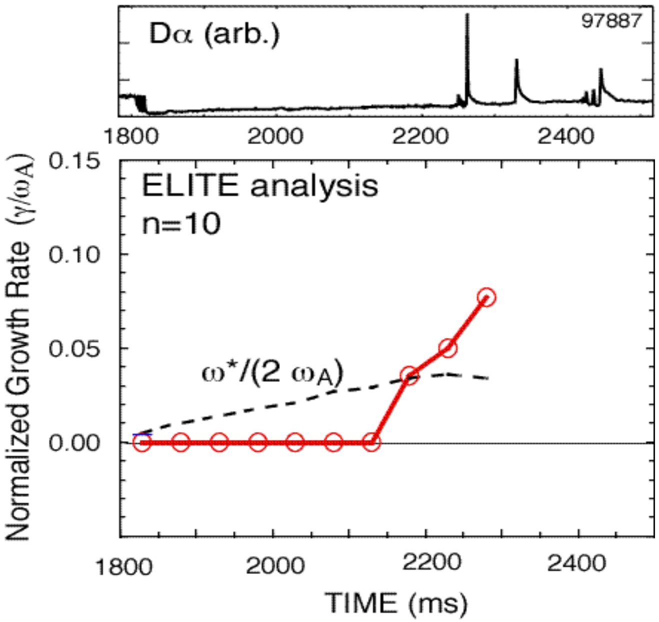

The linear theory can provide quantitative information about *when* the ELM occurs; eg for ELMs on DIII-D [*Snyder, et al*]

one can postulate that ELM energy loss is correlated with radial extent of eigenmode

for example, some evidence from JT60-U but this can only ever be qualitative [*Snyder, et al*]

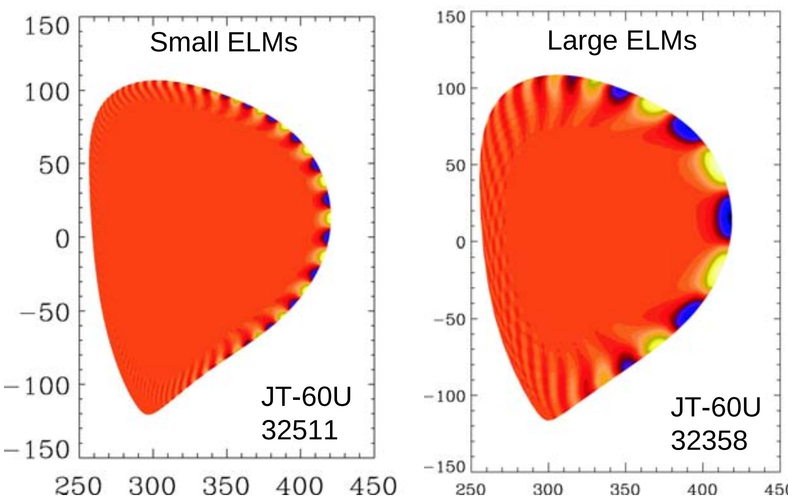

UKAEA Fusion Working in Europe

Ballooning theory and solar eruptions

- A rigorous model for the crash will require a non-linear theory
- Non-linear ballooning theory has previously been explored for understanding solar eruptions *(Hurricane et al)*
- Field lines are "tied" at the two ends, and the theory predicts:
  - explosive growth, even close to linear marginal stability
  - a filament of plasma is ejected
  - reconnection is not a necessary part of the theory
- We explore the predictions of the theory for a tokamak:
  - the theory must be modified to take account of the toroidal geometry
  - the field lines are effectively infinitely long, wrapping many times around the torus
  - can we establish a link between solar eruptions and ELMs?

The linear ballooning mode equation

The ballooning mode equation has the form:

$$L_B\left[\frac{\partial}{\partial\theta},\theta;\mu\frac{dp}{d\psi}\right]H \equiv \frac{d}{d\theta}\left\{\left(1+h(\theta)^2\right)\frac{dH}{d\theta}\right\}+\mu\frac{dp}{d\psi}\left\{\quad g[\theta]+h(\theta)f[\theta]\right\}H(\theta)=\gamma_0^2\left\{1+h(\theta)^2\right\}H(\theta)$$

Functions with square brackets denote equilibrium functions, periodic in θ. At large θ, $h(\theta)\rightarrow s\theta$

Close to marginal stability, we can identify three regions in θ:

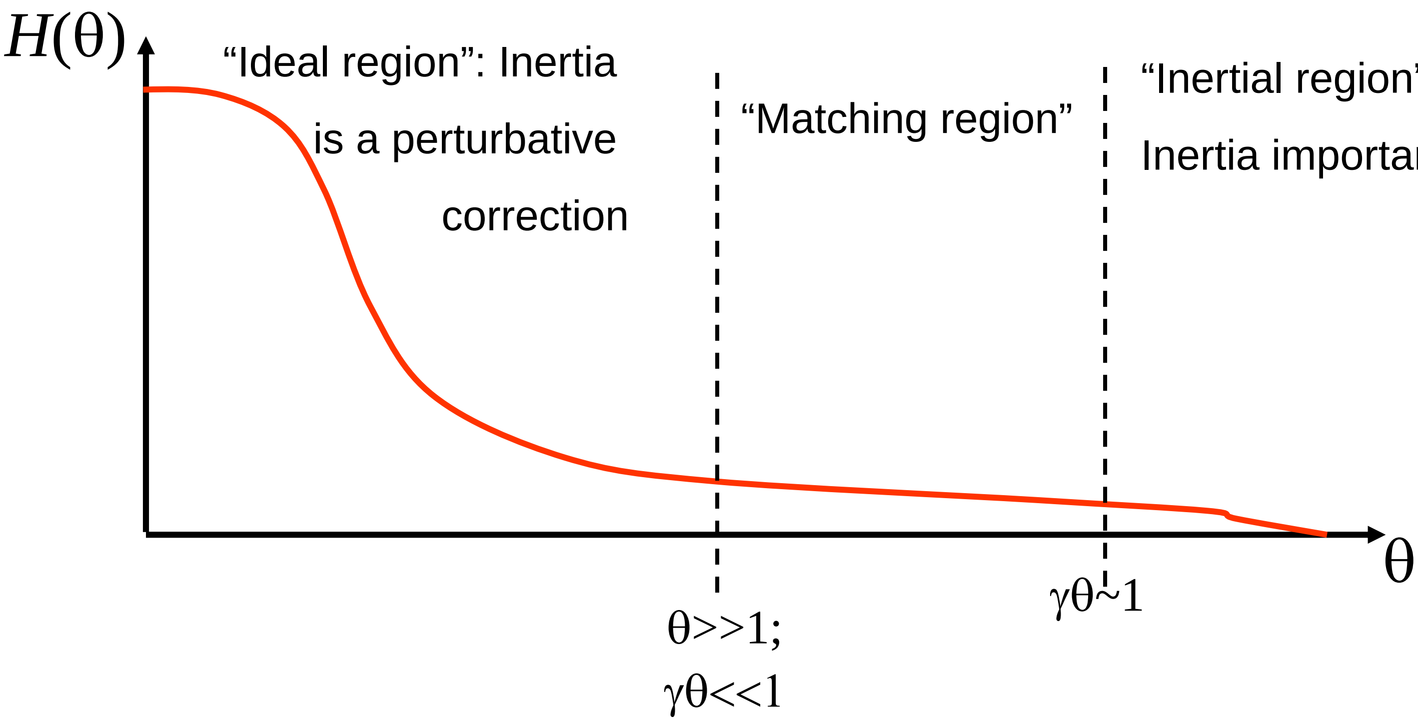

The notion of Δ'

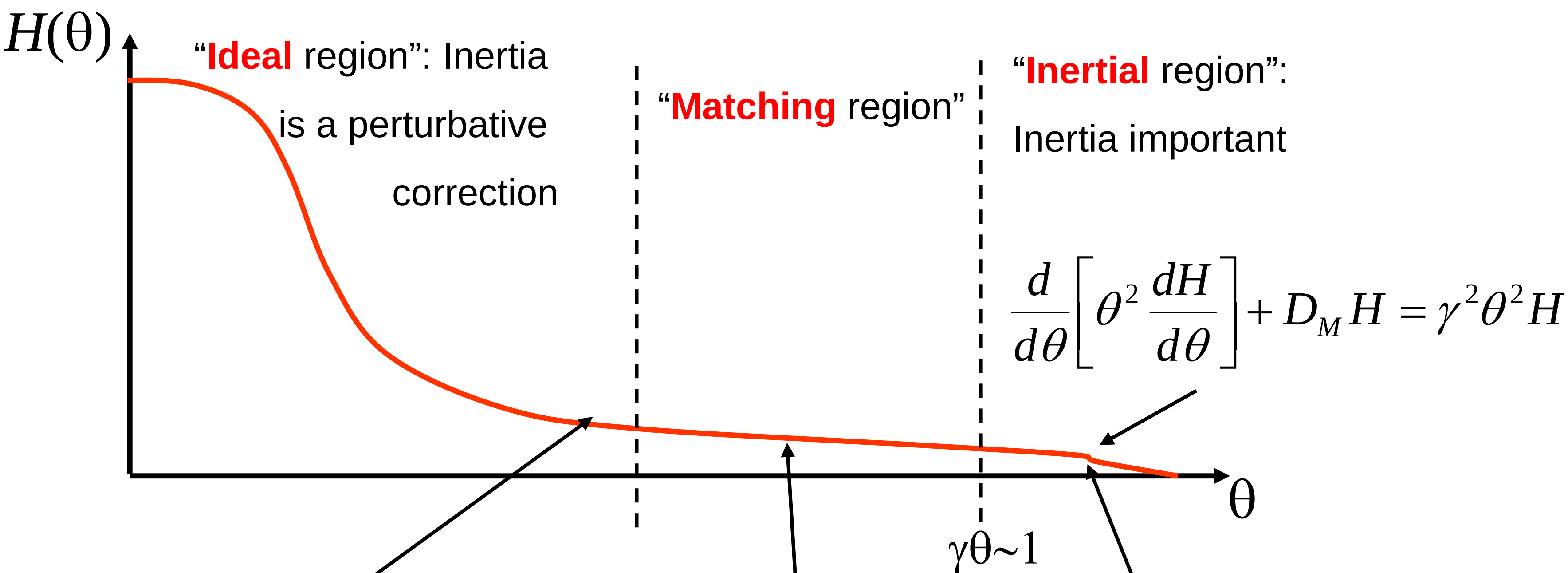

$$H(\theta) = a\left(\frac{1}{\theta^{\lambda_L}} + \frac{\Delta'}{\theta^{\lambda_S}}\right)$$

$$\lim_{\gamma\theta\to 0} H(\gamma\theta) = \hat{a}\left(\frac{1}{(\gamma\theta)^{\lambda_L}} + \frac{b}{(\gamma\theta)^{\lambda_S}}\right)$$

Exponential fall-off

$H=H(\gamma\theta)$

$$\lambda_{S,L} = \frac{1}{2} \pm \sqrt{\frac{1}{4} - D_M}$$

D_M is the Mercier stability index

If we match the two solutions, then we have:

$$\Delta'^{-1} = \frac{\gamma^{\lambda_S - \lambda_L}}{b}$$

The notion of Δ'

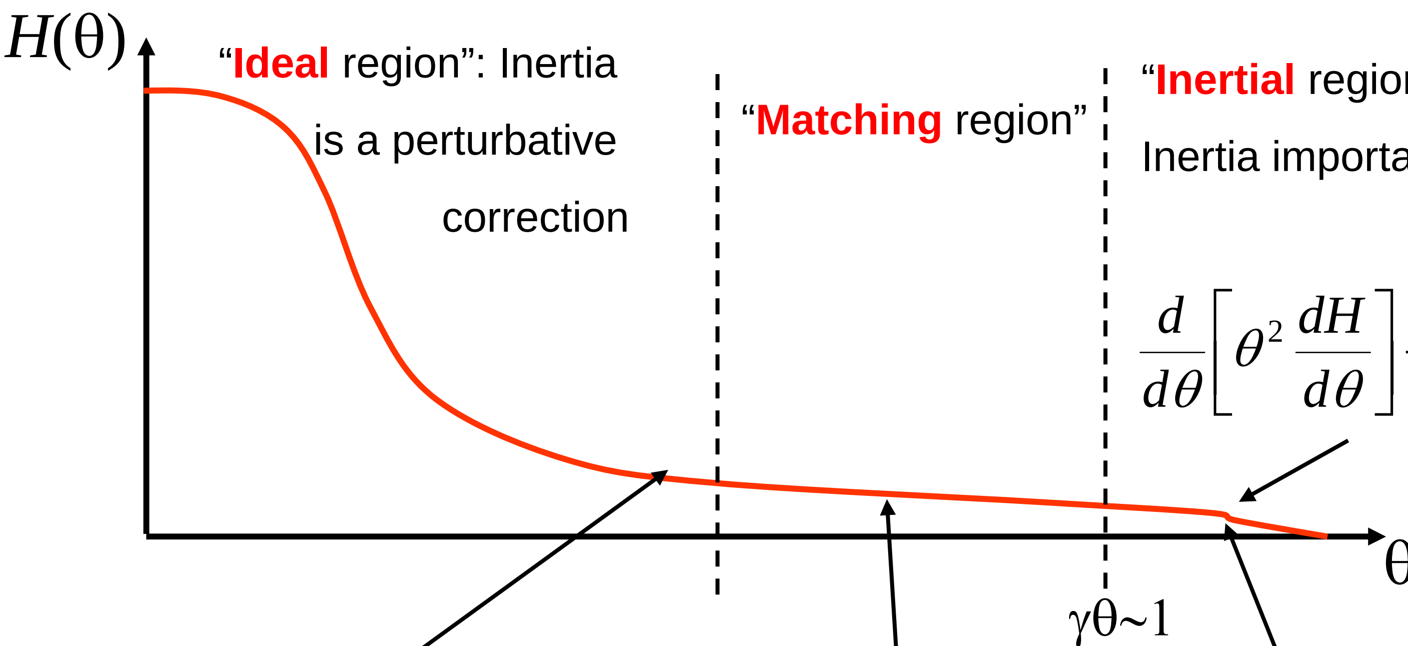

$$\frac{d}{d\theta}\left[\theta^2 \frac{dH}{d\theta}\right] + D_M H = \gamma^2 \theta^2 H$$

$$H(\theta) = a\left(\frac{1}{\theta^{\lambda_L}} + \frac{\Delta'}{\theta^{\lambda_S}}\right)$$

$$\lim_{\gamma\theta\to 0} H(\gamma\theta) = \hat{a}\left(\frac{1}{(\gamma\theta)^{\lambda_L}} + \frac{b}{(\gamma\theta)^{\lambda_S}}\right)$$

Exponential fall-off

$H = H(\gamma\theta)$

$$\lambda_{S,L} = \frac{1}{2} \pm \sqrt{\frac{1}{4} - D_M}$$

D_M is the Mercier stability index

Allowing for the perturbative correction due to γ^2 in the ideal region:

$$\Delta'^{-1} = \Delta_0'^{-1} - \frac{\delta\gamma^2}{\Delta_0'^2} = \frac{\gamma^{\lambda_S - \lambda_L}}{b}$$

Where are non-linearities important?

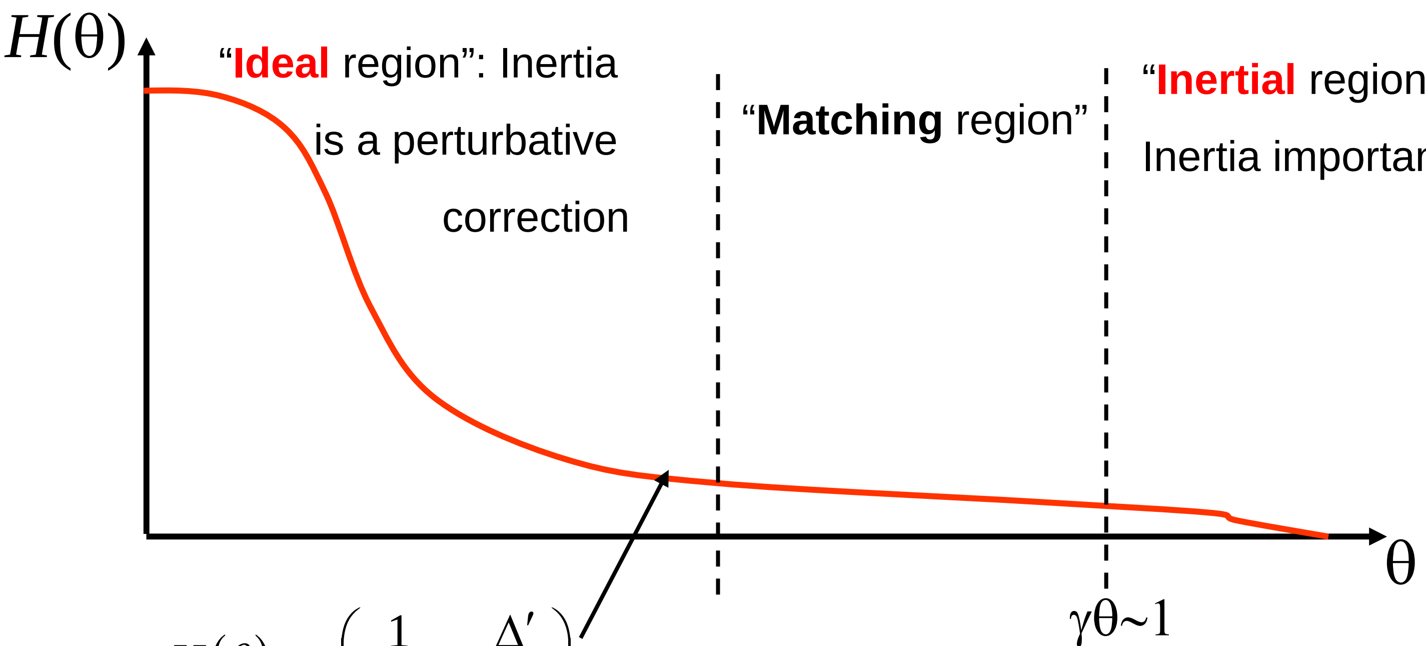

$$H(\theta)=a\left(\frac{1}{\theta^{\lambda_L}}+\frac{\Delta'}{\theta^{\lambda_S}}\right)$$

The "radial" perturbed displacement is

$$\xi=\hat{\xi}(\psi,\alpha)H(\theta)|\mathbf{e}_\perp|\sim\hat{\xi}(\psi,\alpha)\frac{1}{\theta^{\lambda_s-1}}$$

Thus, for $\lambda_s>1$, non-linearities are dominant in the ideal region

For $\lambda_s<1$, non-linearities are dominant in the inertial region

Summary of regions

D_M	$\lambda_s - \lambda_L$	Inertia	Non-linearities
>0 (eg near $q=1$)	$\lambda_s - \lambda_L < 1$	$\sim\gamma^{\lambda s - \lambda L + 2}$ (inertial region)	Dominant in inertial region
$-3/4 < D_M < 0$	$1 < \lambda_s - \lambda_L < 2$	$\sim\gamma^{\lambda s - \lambda L + 2}$ (inertial region)	Dominant in ideal region
$< -3/4$	$\lambda_s - \lambda_L > 2$	$\sim\gamma^2$ (ideal region)	Dominant in ideal region

For $D_M < -3/4$ (strong shaping) line tied boundary conditions are adequate: problem solved by Hurricane et al

For $D_M > 0$ (weak shaping, $q < 1$) this could be relevant for sawtooth: future work

For the pedestal, we are interested in the intermediate regime

Ideal region: The ordering

Starting from the full non-linear ideal MHD equations, we develop an expansion in ε, assuming we are close to marginal stability (ie $\partial/\partial t \ll 1$)

We anticipate an ordering of length scales motivated by the linear theory

$$\frac{\partial}{\partial\theta} = O(1) \qquad \frac{\partial}{\partial\psi} = O(\varepsilon^{-1}) \qquad \frac{\partial}{\partial\alpha} = O(\varepsilon^{-2})$$

note, for linear

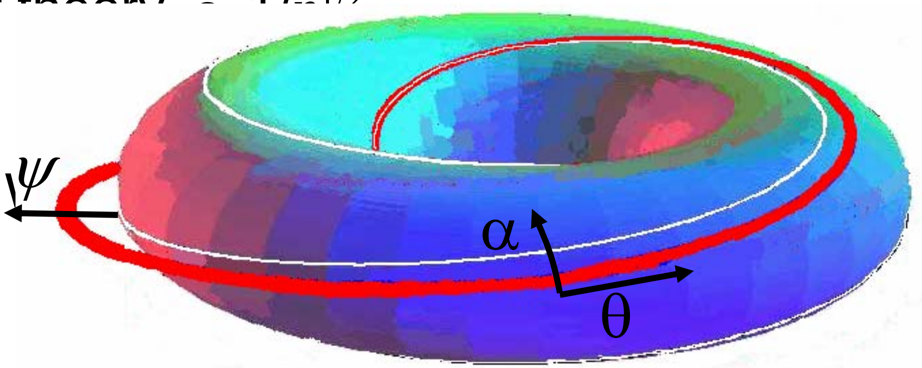

In addition, ψ

$$\xi = O(\varepsilon^{2}) \qquad \frac{\partial}{\partial t} = O(\varepsilon^{\sigma})$$

no “overtaking”; σ is chosen appropriately

Schematic derivation: Ideal region (1)

From the first three orders we find that the radial component of the plasma displacement satisfies the **standard linear ballooning equation:**

$$\xi(\psi,\alpha,\theta,t)=\hat{\xi}(\psi,\alpha,t)H(\theta)$$

$$L_B\left[\frac{\partial}{\partial\theta},\theta;\mu\frac{dp}{d\psi}\right]H=0$$

μ is determined as an eigenvalue, and close to marginal stability, $\mu\approx 1$

NOTE: $H(\theta)$ is not periodic

This is OK provided that the field line does not wrap round on itself before the eigenmode has decayed

Schematic derivation: Ideal region (2)

The fourth order provides useful results, which are used to simplify the fifth order equations

A solubility condition on the fifth order equations provides an equation for Δ' in terms of the envelope function:

$$\frac{1}{\Delta'}\frac{\partial\hat{\xi}}{\partial\alpha}=C_1\left[2(1-\mu)\frac{\partial\hat{\xi}}{\partial\alpha}-C_0\int^{\alpha}d\alpha'\frac{\partial^2\hat{\xi}}{\partial\psi^2}\right]+C_2\frac{\partial\hat{\xi}^2}{\partial\alpha}+C_4\frac{\partial\hat{\xi}}{\partial\alpha}\frac{\partial^2\overline{\hat{\xi}^2}}{\partial\psi^2}$$

The coefficients are derived from averages along the field line of functions involving $H(\theta)$:

the C_2 coefficient is logarithmically divergent as $D_M\rightarrow 0$ (low β, large aspect ratio, circular cross-section)

Inertial region

The inertial region is characterised by $\theta >> 1$; $\theta\, \partial/\partial t \sim 1$

The perturbations are described by linear equations

In this region we can average out short-scale (periodic) θ variation and Laplace-transform perturbed quantities:

$$\hat{X}(p) = \int_0^\infty e^{-pt} X(t)\, dt$$

The small $\theta\, \partial/\partial t$ limit of the Laplace-transformed equations provides another expression for Δ' which, after inverting the Laplace transform, becomes:

$$\frac{\hat{\xi}(t)}{\Delta'(t)} = \frac{b}{2\pi i} \frac{\partial^2}{\partial t^2} \left[\int_0^\infty dt' \hat{\xi}(t') \int_{-i\infty+\tau_0}^{i\infty+\tau_0} dp\; p^{d-2} e^{p(t-t')} \right] = \Gamma(2 + \lambda_L - \lambda_S) \frac{\partial^2}{\partial t^2} \left[\int_0^t dt' \frac{\hat{\xi}(t')}{(t-t')^{\lambda_S - \lambda_L - 1}} \right]$$

A representation of a fractional derivative

τ_0 is a small positive time; $1 < d = \lambda_s - \lambda_L < 2$

The final equation:

We can now equate the two expressions for Δ' obtained from the two regions to derive our final result:

Contribution from inertial region

A representation of a fractional derivative

$$\Gamma(2+\lambda_L-\lambda_S)\frac{\partial}{\partial\alpha}\frac{\partial^2}{\partial t^2}\left[\int_0^t dt'\frac{\hat{\xi}(t')}{(t-t')^{\lambda_S-\lambda_L-1}}\right]=$$

Non-linear drive term

$$C_1\left[2(1-\mu)\frac{\partial\hat{\xi}}{\partial\alpha}-C_0\int^{\alpha}d\alpha'\frac{\partial^2\hat{\xi}}{\partial\psi^2}\right]+C_2\frac{\partial\hat{\xi}^2}{\partial\alpha}+C_4\frac{\partial\hat{\xi}}{\partial\alpha}\frac{\partial^2\overline{\hat{\xi}^2}}{\partial\psi^2}$$

Linear instability drive

“Finite n” linear term (stabilising)

Cubic non-linearity determines radial structure

Form of solution: time dependence

We balance the non-linear drive with inertia, to predict explosive growth as the time t approaches t_0:

$$\hat{\xi}(t) \sim \frac{1}{\left[t_0(\alpha,\psi)-t\right]^{\lambda_S-\lambda_L}} \qquad 1<\lambda_S-\lambda_L<2; \quad -3/4<D_M<0$$

$$\hat{\xi}(t) \sim \frac{1}{\left[t_0(\alpha,\psi)-t\right]^{2}} \qquad \lambda_S-\lambda_L>2; \quad D_M < -3/4$$

Favours a given α, ie that for which t_0 is a minimum.

Form of solution: spatial structure

To understand spatial structure, consider our solution:

$$\hat{\xi}(t) \sim \frac{1}{[t_0(\alpha,\psi)-t]^{\lambda_S-\lambda_L}}$$

Balancing the two non-linear terms, we find radial width broadens while the extent in α narrows:

$$\frac{(\Delta\psi)^2}{\Delta\alpha} \sim \frac{1}{(t_0-t)^{\lambda_S-\lambda_L}}$$

Numerical solution confirms these features:

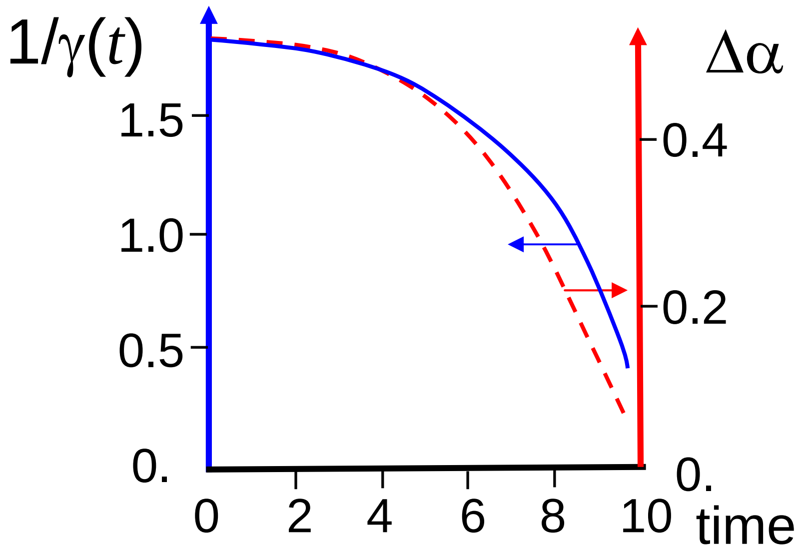

$\lambda_s - \lambda_L = 1.6$

A picture of the non-linear ballooning mode

Our picture of a non-linear ballooning mode is the following:

Field line unperturbed on inboard side
$\Rightarrow$ remains connected into the core plasma

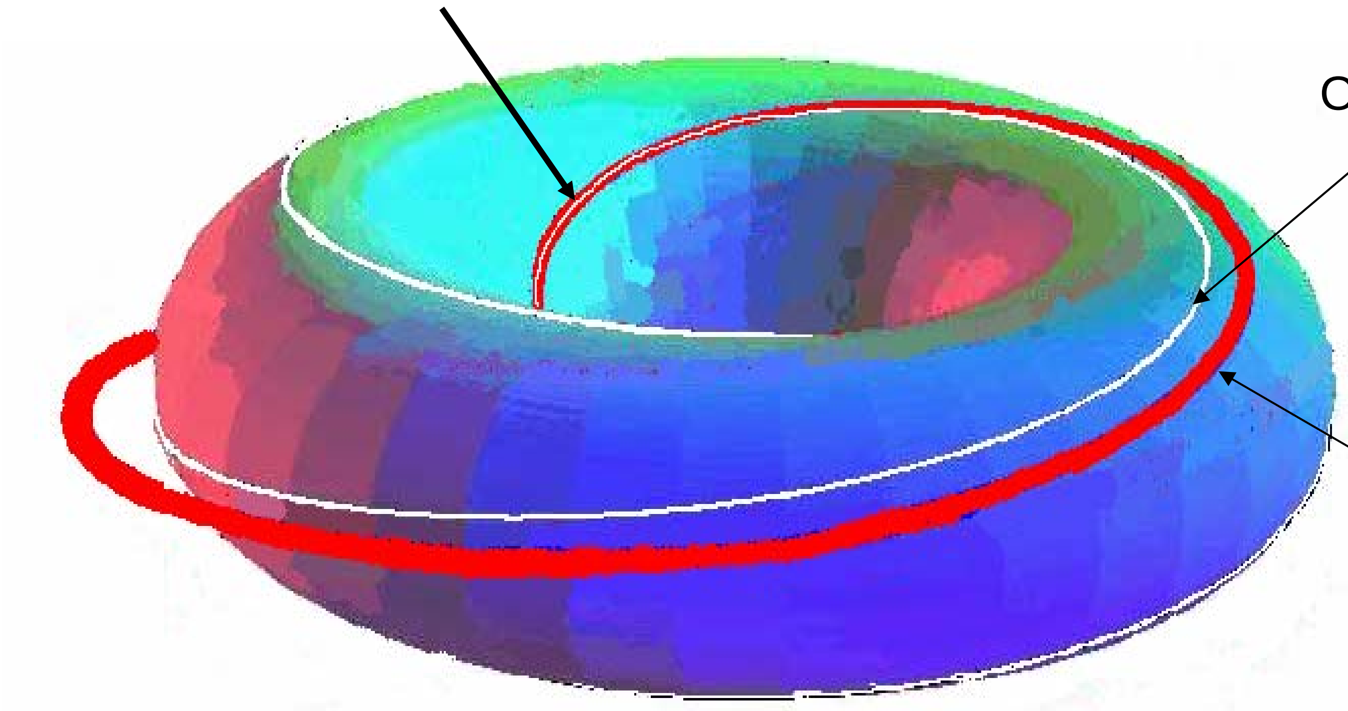

Original field line position

Ballooning mode pulls field line out on outboard side

Non-linear MHD code, BOUT, shows similar feature

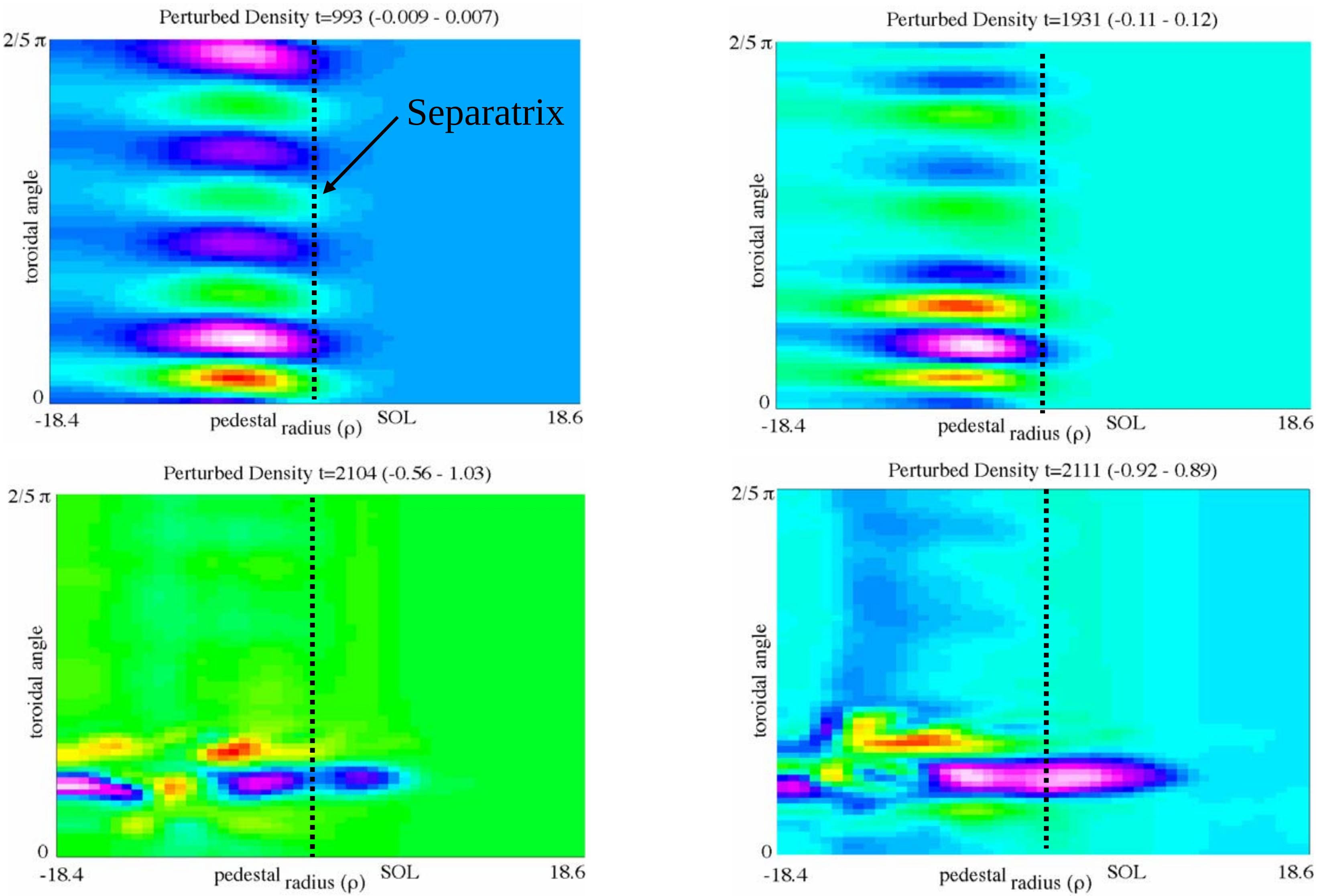

- R,ϕ plots on outer midplane. Linear phase, n=20. Burst occurs asymmetrically at a particular toroidal location. “Finger” is an extended filament along the field - similarities to observations (MAST, DIII-D) and nonlinear ballooning theory

P B Snyder, EPS 2004

GENERAL ATOMICS

A photograph of a MAST ELM

Filament erupting from the surface of the MAST plasma

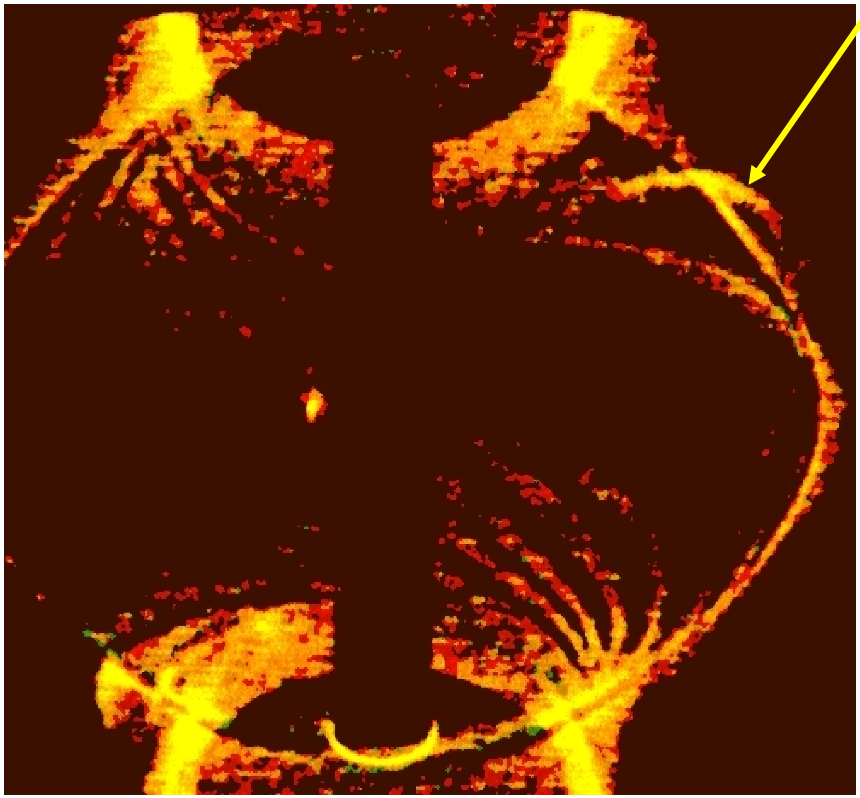

A Kirk, R Akers

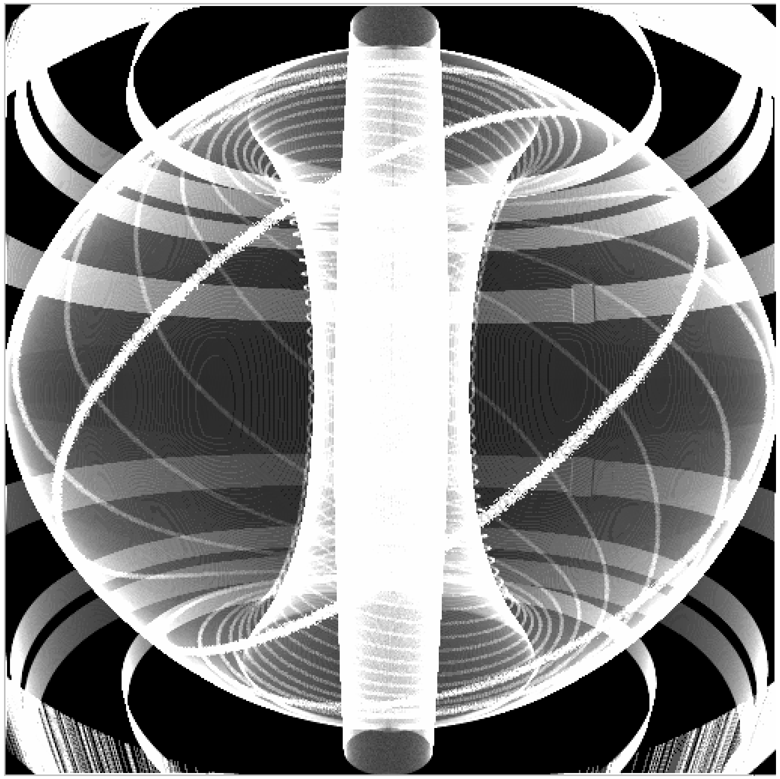

Reconstruction of the MAST magnetic geometry, with 10 field lines highlighted

- Since the MAST observation last year, experimentalists have searched for, and found, filamentary structures on ASDEX Upgrade, JET and DIII-D

A picture of the ELM

- As the pedestal pressure (and current) build, the linear stability threshold is crossed
- The ballooning mode ejects a hot plasma filament into the scrape-off layer plasma on the outboard side
- This filament remains connected into the hot core on the inboard side:
  - it provide a “hosepipe” through which hot plasma can drain from the core
  - if this filament were to strike the vessel wall on ITER it could do damage
  - this theory could, therefore, have significant implications for ITER
- The heat and particles must somehow leave the pedestal and enter the scrape-off layer
  - goes beyond ideal MHD
  - what is the role of the filaments in this process?

Do the filaments cause heat/particle loss?

- Could heat/particles escape from the filament into the SOL?
  - Recall that the filament narrows as it evolves
    - enhanced radial diffusion
  - Hot filament in “cold” SOL plasma likely leads to “secondary” instabilities
    - These could further enhance the transport from the filaments into the SOL
  - Subject of future research
- But there is another possibility:
  - The filament must twist to squeeze between field lines on adjacent surfaces
  - It can only do this if the shear in the flow is suppressed
    - Does the ballooning mode suppress the shear flow, or does the flow suppress the ballooning mode?
  - If the sheared flow is suppressed, one would expect a transition to L-mode

Coupled Transport-MHD Model: Towards an integrated ELM model

- Essential ingredients:
  - Transport model for inter-ELM period
  - Couple to ideal MHD code to determine
    - Instability threshold
    - Mode structure
  - Provide a crash model
    - Option (1):
      - Barrier transport reverts to L-mode in region of instability (filament suppresses flow)
      - Enhanced transport for characteristic time of explosive event
      - This seems do-able in the near term
    - Option (2)
      - Identify transport processes of heat and particles out of filament
      - Will require long-term development
    - This would still leave us with a need to understand the impact of the kink/peeling component
  - SOL transport model

Summary

To understand the ELM crash dynamics, requires the integration of several plasma processes

Transport to model the post-ELM recovery

Linear MHD stability analysis to determine the ELM trigger

Non-linear MHD analysis to determine ELM structure

Novel theory to describe the impact of the filaments

SOL transport to predict heat loads at the target plates and/or wall

A complete ELM model is clearly a challenging task:

this should remain our vision, and we are making progress

in the meantime, there are useful models that can be adopted and developed to at least test some aspects